EurJIC European Journal of Inorganic Chemistry

FULL PAPER

DOI: 10.1002/ejic.201200387

Nucleophilic Addition Reactions of the Nitroprusside Ion – The Case of *O*-Methylhydroxylamine

María M. Gutiérrez,[a] José A. Olabe,[b] and Valentín T. Amorebieta*[a]

Keywords: Amines / Nucleophilic addition / Kinetics / Density functional calculations / Iron

The kinetics of the reaction between aqueous solutions of $[Fe(CN)_5NO]^{2-}$ and NH_2OCH_3 has been studied by means of UV/Vis spectroscopy and complementary solution techniques, FTIR/ATR spectroscopy, mass spectrometry, and isotopic labeling ($[Fe(CN)_5{}^{15}NO]^{2-}$), in the pH range 6.0–9.3, I = 1 M (NaCl). The main products were nitrous oxide ($N^{15}NO$), CH_3OH, and $[Fe^{II}(CN)_5H_2O]^{3-}$, characterized as the $[Fe^{II}(CN)_5(pyCONH_2)]^{3-}$ complex ($pyCONH_2$ = isonicotinamide). In excess NH_2OCH_3, the kinetic runs indicated pseudo-first-order behavior, with corresponding rate constants, k_{obs} [s^{-1}], that correlated linearly with the concentration of NH_2OCH_3. The rate law is: $R = k_{exp}[Fe(CN)_5NO^{2-}][NH_2OCH_3]$, with k_{exp} = $(4.1 \pm 0.4) \times 10^{-4}$ $M^{-1}s^{-1}$ at 25 ± 0.2 °C, $\Delta H^{\#}$ = 27 ± 1 kJ mol^{-1}, and $\Delta S^{\#}$ = –220 ± 5 J K^{-1} mol^{-1}, at pH 7.1. The value of k_{exp} is much lower than that for similar addition reactions of NH_2OH and of the *N*-substituted methyl derivative. In addition, the latter reactions exhibit a third-order rate law with a linear dependence of R on the concentration of OH^-. The reaction profile has been modeled by density functional theoretical methodologies, providing mechanistic evidence on the different reaction steps, namely, the adduct formation and subsequent decomposition processes, with valuable comparisons with the reactivity of other nucleophiles with $[Fe(CN)_5NO]^{2-}$.

Introduction

The mechanisms of the reactions of the small molecules involved in the nitrogen redox cycles are of general interest, both from the fundamental and applied points of view.[1] Within the broad scope of this field, a common feature deals with the necessary coordination at a transition metal center for the adequate activation of the substrates. An example of this chemistry is represented by the nitrosyl group,[2] which includes a role for stabilized metal–NO moieties that behave as crucial intermediates in the reactivity of NO_2^-. The nitroprusside ion, $[Fe(CN)_5NO]^{2-}$, is an electrophile toward a variety of substrates,[3] reacting with N-binding nucleophiles such as NH_3[4] and NH_2R,[5] NH_2OH,[6] N_2H_4,[7] as well as with others like OH^-,[8] HS^-,[9] and thiolates.[10] In this way, different reduction products of NO^+ can be obtained.

Within the scope of the chemistry of hydroxylamines,[11] others and we have dealt either with the disproportionation reactions[12] or with the addition reactions to the nitrosonium ligand.[6,13] NH_2OH is a product of mammalian biosynthesis,[14] and its consumption may be expected to proceed through such a type of mechanistic routes. We reported on the kinetics of the reaction of $[Fe(CN)_5NO]^{2-}$ with the also bioinorganically relevant *N*-methylhydroxylamine, $NH(CH_3)OH$,[13] with complementary evidence that the disubstituted derivative, *N*,*N*′-dimethylhydroxylamine, is not reactive. Thus, by introducing methyl substituents on NH_2OH, we found significant stoichiometric and mechanistic changes in the addition reactions, which are interesting in their own right.

In this work, we extend the studies to the reaction of $[Fe(CN)_5NO]^{2-}$ with *O*-methylhydroxylamine (NH_2OCH_3) by using detailed kinetic methodologies, including isotope labeling of the nitrosyl group and DFT calculations. NH_2OCH_3 is suitable for preparing *O*-alkyloximes and *O*-alkylhydroxamates, which are intermediates for the production of antibiotics and oxime-type herbicides. In addition, NH_2OCH_3 serves as a reagent for the protection and derivatization of keto groups in steroids, in order to detect sugars and amino sugars in glycoproteins. It constitutes an active ingredient in several drugs for the treatment of diabetes and for the development of new anticancer therapies.[15] The presently reported results add to the previously considered calculations on the addition reactivities and subsequent decompositions when other nitrogen hydrides react with $[Fe(CN)_5NO]^{2-}$,[16] allowing for fruitful mechanistic comparisons.

[a] Department of Chemistry, Facultad de Ciencias Exactas y Naturales, Universidad Nacional de Mar del Plata, Funes y Roca, Mar del Plata B7602AYL, Argentina
E-mail: amorebie@mdp.edu.ar
Homepage: www.mdp.edu.ar
[b] Department of Inorganic, Analytical and Physical Chemistry and INQUIMAE/CONICET, Facultad de Ciencias Exactas y Naturales, Universidad de Buenos Aires, Ciudad Universitaria, Pabellón 2, Buenos Aires C1428EHA, Argentina
Supporting information for this article is available on the WWW under http://dx.doi.org/10.1002/ejic.201200387.

 © 2012 Wiley-VCH Verlag GmbH & Co. KGaA, Weinheim

Results and Discussion

The stoichiometry of products shows the formation of N_2O and CH_3OH, as revealed by the analysis made in the reactor headspace and in the exhausted mixtures, in excess NH_2OCH_3 (≥ 10). The conversion of $[Fe^{II}(CN)_5NO]^{2-}$ into $[Fe^{II}(CN)_5pyCONH_2]^{3-}$ is essentially quantitative, with a yield greater than 95%. Independent measurements of the number of mol of N_2O and CH_3OH indicate a 1:1 ratio, with a yield also nearly quantitative with respect to the initial $[Fe^{II}(CN)_5NO]^{2-}$. The molar concentration of N_2O in the condensed phase and the gas pressure, $p_g = p$(measured) – p(vap., H_2O), are related by: $[N_2O] = p_g(V_g/V_L + 1/H)/(RT)$. $H = n(N_2O, g)V_L/(n(N_2O, L)V_g) \approx 1.6$, is the dimensionless Henry constant. $n(N_2O, g)$, $n(N_2O, L)$, V_g, and V_L are the mol of N_2O and the volumes of the gaseous and condensed phases, respectively.

Starting with $[Fe^{II}(CN)_5{}^{15}NO]^{2-}$, the mass spectrum of nitrous oxide showed the fragment ions at m/e = 45 and 31 and relative abundances of 100 to about 30. This is evidence of $N^{15}NO$ formation[17] and confirms the absence of the alternative isomer, ^{15}NNO, with characteristic ions at m/e = 45 and 30. On the other hand, in the reaction with unlabeled $Na_2[Fe(CN)_5NO]\cdot 2H_2O$ (SNP), the m/e values of the fragments were 44 and 30, with relative intensities as before. Thus, the final products, generated in a molar ratio of 1:1:1, were $N^{15}NO$, CH_3OH, and $[Fe(CN)_5(pyCONH_2)]^{3-}$. We found no evidence of reaction intermediates during the UV/Vis spectral evolution, or during the FTIR/ATR and EPR spectroscopic analyses, even when the reaction evolved under substoichiometric NH_2OCH_3 conditions. In the IR spectroscopic experiments, the distinctive observation was that the stretching absorptions of SNP (ν_{CN} and ν_{NO} at about 2140 and 1935 cm^{-1}, respectively)[18] were replaced by a broad band centered at about 2040 cm^{-1}, characteristic of $[Fe^{II}(CN)_5L]^{3-}$ complexes (L = CN^-, $pyCONH_2$, DMSO, etc.).[19] Equations (1) and (2) describe the main reaction stoichiometry with labeled $[Fe(CN)_5{}^{15}NO]^{2-}$.

$$[Fe(CN)_5{}^{15}NO]^{2-} + NH_2OCH_3 + OH^- \rightarrow [Fe(CN)_5H_2O]^{3-} + N^{15}NO + CH_3OH \quad (1)$$

$$[Fe(CN)_5H_2O]^{3-} + pyCONH_2 \rightarrow [Fe(CN)_5(pyCONH_2)]^{3-} + H_2O \quad (2)$$

Equation (2) describes the trapping procedure employed for excluding $[Fe^{II}(CN)_5H_2O]^{3-}$ from the reaction medium (thus precluding its catalytic role in the disproportionation of NH_2OCH_3).[12c] It has been independently measured by stopped-flow techniques, with k_2 = 296 $M^{-1}s^{-1}$ at 25 °C.[20] Under the selected working conditions, reaction (2) proceeds several orders of magnitude faster than reaction (1).

Table 1 shows the results of the kinetic studies performed under pseudo-first-order conditions in NH_2OCH_3 and at different pH values. Most of the runs involved the spectroscopic detection of $[Fe(CN)_5(pyCONH_2)]^{3-}$ [Equation (2)]. As the reaction is very slow, we routinely used the initial rate method.[21] Nevertheless, some runs performed to completion showed a satisfactory first-order buildup of $[Fe^{II}(CN)_5(pyCONH_2)]^{3-}$ or N_2O. The first-order rate constants, k_{obs}, displayed a linear dependence on the analytical concentration of NH_2OCH_3, yielding the second-order rate constants, k_{exp}. Thus, the observed rate law is $R\,[M\,s^{-1}] = k_{exp}[Fe(CN)_5NO^{2-}][NH_2OCH_3]$, with $k_{exp} = (4.1 \pm 0.4) \times 10^{-4}$ $M^{-1}s^{-1}$, at 25 ± 0.2 °C. Figure S1 shows the plot for calculating the activation parameters: $\Delta H^{\neq}_{exp} = 27 \pm 3$ kJ mol^{-1} and $\Delta S^{\neq}_{exp} = -220 \pm 10$ J K^{-1} mol^{-1}.

Table 1. Rate constants for the reaction between $[Fe(CN)_5NO]^{2-}$ and NH_2OCH_3, at different concentrations and pH values; I = 1 M (NaCl), 25 ± 0.2 °C; measured through the build-up of $[Fe^{II}(CN)_5(pyCONH_2)]^{3-}$, unless otherwise indicated.

pH	[SNP] [mM]	$[NH_2OCH_3]$ [mM]	$10^6 \times k_{obs}$ [s^{-1}]	$10^4 \times k_{exp}$ [$M^{-1}s^{-1}$]
9.3	7.7	57.0	23.4	4.1
9.3	2.0	59.0	22.4	3.8
9.3	2.0	80.0	34.4	4.3
9.3	2.0	20.0	7.8	3.9
9.3	14	140	61.6	4.4[a]
9.3	16.4	246.0	95.9	3.9
8.5	2.0	80.0	29.6	3.7[b]
8.0	0.31	12.2	4.6	3.8
8.0	1.1	14.9	6.1	4.1
8.0	1.1	23.3	9.8	4.2
7.1	2.0	80.0	33.6	4.2
7.1	1.0	22.0	8.6	3.9
7.1	2.0	20.0	9.0	4.5
7.1	1.0	9.7	4.1	4.2
6.0	1.0	22.0	8.8	4.0
6.0	1.0	9.7	3.8	3.8
6.0	0.9	45.0	20.3	4.5
6.0	4.9	23.0	8.5	3.7

[a] Monitored through the production of N_2O. [b] Monitored by FTIR/ATR spectroscopy at 1935 cm^{-1}.

In view of the overall stoichiometry described by Equation (1), we conclude that the studied reaction is complex. The negative entropy of activation is consistent with an initial associative process between the reactants. However, its value is much more negative than those for other nucleophiles (see below, Table 3). Generally, these reactions comprise reversible additions of the nucleophiles to $[Fe(CN)_5NO]^{2-}$ with the formation of an adduct and subsequent decompositions. We propose the same for the reaction of NH_2OCH_3 [Equation (3)]. Adduct formation is followed by the migration of one hydrogen atom, bound to the nitrogen atom of NH_2OCH_3, to the oxygen atom of the nitrosyl group, which leads to the intermediate $[Fe(CN)_5N(OH)N(H)OCH_3]^{2-}$ [Equation (4)]. The decomposition of this intermediate leads to the reaction products.

$$[Fe(CN)_5{}^{15}NO]^{2-} + NH_2OCH_3 \rightleftarrows [Fe(CN)_5{}^{15}N(O)NH_2OCH_3]^{2-}\ k_3, k_{-3} \quad (3)$$

$$[Fe(CN)_5{}^{15}N(O)NH_2OCH_3]^{2-} \rightleftarrows [Fe(CN)_5{}^{15}N(OH)N(H)OCH_3]^{2-}\ k_4, k_{-4} \quad (4)$$

We do not rule out a previous pre-equilibrium between the reactants leading to an encounter-complex transient.[3a] For clarity, and for highlighting the significance of labeling

 © 2012 Wiley-VCH Verlag GmbH & Co. KGaA, Weinheim

in the identification of the structure of product N_2O, we designate the nitrosyl group in the chemical equations as ^{15}NO.

Figure 1 depicts the energy profile along the reaction path and the optimized structures of the dynamically stable species, according to DFT calculations. For simplicity, we do not show the optimized structures of the reactants and reaction products. The first reaction step comprises the formation of an intermediate, labeled as I1, through the transition state TS1. The structure of I1 differs from that of the product of reaction (4) in the position of the hydrogen atom bound to the oxygen atom of the nitrosyl group. In $[Fe(CN)_5N(OH)N(H)OCH_3]^{2-}$, this hydrogen atom is closer to the nitrogen atom of the nitrosyl, whilst in I1 it is in close proximity to the oxygen atom of the CH_3O group, as a result of an activated rotation. We describe this process by Equation (5).

$$[Fe(CN)_5{}^{15}N(OH)N(H)OCH_3]^{2-} \rightleftarrows I1 \; k_5, k_{-5} \quad (5)$$

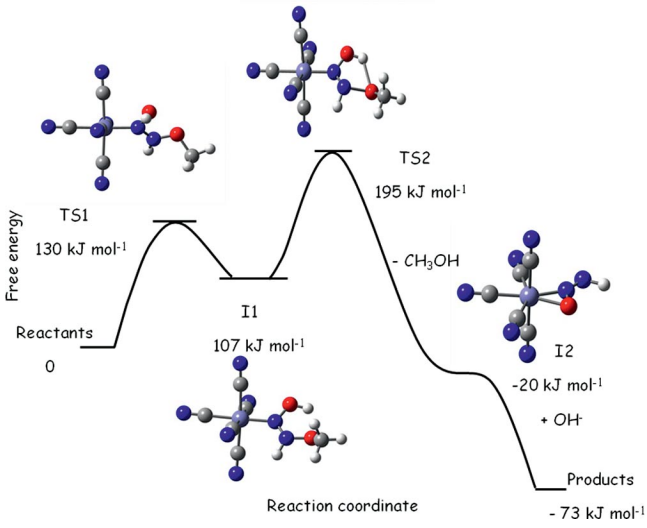

Figure 1. Reaction profile, with changes in Gibbs free energy, and schematic representation of the optimized structures involved in the reaction between $[Fe(CN)_5NO]^{2-}$ and NH_2OCH_3. Small light gray spheres represent H atoms, gray spheres C, blue spheres N, red spheres O, and light blue spheres Fe.

From the calculations, we obtain a positive change in the free energy of formation for the adduct and for $[Fe(CN)_5{}^{15}N(OH)N(H)OCH_3]^{2-}$. However, we could not find the transition states associated with the formation of these species. This may be due to convergence problems of the model or because the decomposition of the adduct and $[Fe(CN)_5N(OH)N(H)OCH_3]^{2-}$ (steps –3 and –4) have a low activation energy. Then, instead of the three steps involved in Equations (3)–(5), we may consider only one reaction for describing the formation of I1, as shown in Equation (6).

$$[Fe(CN)_5{}^{15}NO]^{2-} + NH_2OCH_3 \rightleftarrows I1 \; k_6, k_{-6} \quad (6)$$

During the formation of I1, the Fe–N–O angle changes from its value of about 180° in $[Fe(CN)_5NO]^{2-}$ to 125–130°, a typical linear-to-bent transformation in the {FeNO} moiety.[2,3,16] The bonds Fe–N and N–O elongate relative to those in $[Fe(CN)_5NO]^{2-}$, revealing a strong decrease in the bond orders. The Fe–C and C–N bond lengths do not change significantly upon the formation of I1, showing that the reactivity is mainly associated with changes in the {FeNO} fragment.[16]

We may consider two possible routes for the decomposition of I1: (a) an attack of OH^- with water production, that is, a proton transfer to the medium; (b) an intramolecular transfer of a hydrogen atom to the CH_3O moiety, subsequent O–N bond cleavage, and release of CH_3OH. Since the global reaction is pH-independent, we favor the second route for the calculations [Equation (7)]. As shown in Figure 1, the decomposition of I1 is an activated process. The transition state for the transformation, TS2, has a cyclic optimized structure [O–N–N–O–H]. After generating CH_3OH, the reaction proceeds through intermediate I2, in which the nitrous oxide precursor binds in an η^2-mode.[16] Finally, the exergonic process of product formation is described by Equations (8) and (9), comprising nonactivated processes for the conversion of I2 into N_2O and $[Fe(CN)_5H_2O]^{3-}$. Table 2 shows a complete set of calculated thermodynamic parameters corresponding to the steps displayed in Figure 1.

$$I1 \rightarrow [Fe(CN)_5(^{15}NO)NH]^{2-} + CH_3OH \; k_7 \quad (7)$$

$$[Fe(CN)_5(^{15}NO)NH]^{2-} + OH^- \rightarrow [Fe(CN)_5N^{15}NO]^{3-} + H_2O \; k_8 \quad (8)$$

$$[Fe(CN)_5 N^{15}NO]^{3-} + H_2O \rightarrow [Fe(CN)_5H_2O]^{3-} + N^{15}NO \; k_9 \quad (9)$$

Table 2. Relevant thermodynamic properties at 298 K and 1 bar, obtained by DFT calculations with the isodensity polarizable continuous model (IPCM) approximation, for the reaction between $[Fe(CN)_5NO]^{2-}$ and NH_2OCH_3.

Reaction path	ΔH [kJ mol^{-1}][a]	ΔS [J K^{-1} mol^{-1}][a]
Reactants to TS1	81	–164
TS1 to I1	–25	–8
I1 to TS2	86	–6
TS2 to I2	–141	251
I2 to products	–71	–62
Reactants to products	–69	11

[a] These represent changes in the thermodynamic properties of activation or of reaction, as appropriate. The correction for the zero-point energies was properly considered.

By applying the steady-state approximation to I1 in Equations (6) and (7), we obtain the following rate law: $R = -k_7[I1] = [K_6k_7/(1 - k_7/k_{-6})[Fe(CN)_5{}^{15}NO^{2-}][NH_2OCH_3]$. If $1 >> (k_7/k_{-6})$, the rate constant becomes: $k_{theor} = K_6k_7 = (k_BT/h)\exp(-\Delta G_{theor}/RT)$. To explore the temperature profile of the composite rate constant, k_{theor}, we write a transition state equation for the rate constant k_7 and the van 't Hoff equation for the equilibrium constant K_6. The values of the thermodynamic properties associated with rate and equilibrium constants are symbolized with the superscripts ≠ and 0, respectively. Thus, from the DFT calculations reported in Table 2: $\Delta G_{theor} = \Delta G^0{}_6 + \Delta G^{\neq}{}_7 = \Delta H_{theor} - (T\Delta S_{theor})$, with $\Delta H_{theor} = (\Delta H^0{}_6 + \Delta H^{\neq}{}_7) = 56 + 86 = 142$ kJ mol^{-1} and $\Delta S_{theor} = (\Delta S^0{}_6 + \Delta S^{\neq}{}_7) = -172 -$

 © 2012 Wiley-VCH Verlag GmbH & Co. KGaA, Weinheim

6 = –178 J K^{-1} mol^{-1}. Comparing the results with the experimental values, we predict a highly negative entropic change, though the activation enthalpy is overestimated.[22]

In studies of OH^- as a nucleophile reacting with a broad set of nitrosyl complexes (MNO^+), we found that the rate constants correlated with the MNO^+/MNO redox potentials.[23] Thus, it is proposed that the second-order rate law reflects the nucleophilic addition step forming the MNO_2H adduct, which rapidly deprotonates to NO_2^-. A similar picture occurred with the reactions of $[Fe(CN)_5NO]^{2-}$ with HS^-, cysteine, and related thiolates.[9,10] In these processes, the adducts are moderately stable, because the decomposition steps (either the dissociation of NO_2^- or the redox decay of NOSR) are slow. Table 3 shows the results for OH^-, SH^-, and cysteine; the sulfur compounds add faster, presumably because of their greater polarizability. In addition, we can see that the values of the activation entropies are in the range from –50 to –100 J K^{-1} mol^{-1}. For nucleophiles NH_2OH or $NHCH_3OH$, Equations (10) and (11) describe the stoichiometries. A distinctive, pH-dependent rate law has been found: $R = k_{exp}\ [Fe(CN)_5NO^{2-}][Nucl][OH^-]$.

$$[Fe(CN)_5{}^{15}NO]^{2-} + NH_2{}^{18}OH + OH^- \rightarrow [Fe(CN)_5H_2O]^{3-} + {}^{15}NN^{18}O + H_2O \quad (10)$$

$$[Fe(CN)_5{}^{15}NO]^{2-} + NHCH_3OH + OH^- \rightarrow [Fe(CN)_5H_2O]^{3-} + CH_3N({}^{15}NO)OH + H_2O \quad (11)$$

Table 3. Experimental rate constants and activation parameters for the addition of different nucleophiles to the $[Fe(CN)_5NO]^{2-}$ ion.[a]

Nucleophile	k_B [M^{-1} s^{-1}]	$\Delta H^{\neq}$ [kJ mol^{-1}]	$\Delta S^{\neq}$ [J K^{-1} mol^{-1}]	Ref.
$NH_2C_2H_5$	5.1×10^{-3}[b]	15	–239	[5]
$NH_2C_3H_7$	5.9×10^{-3}[b]	20	–218	[5]
N_2H_4	0.43[c]	27	–163	[7]
NH_2OCH_3	4.1×10^{-4}	27	–220	this work
NH_2OH	0.45[d]	37[c]	–13[c]	[6]
$NH(CH_3)OH$	0.16[d]	34	–32	[13]
OH^-	0.55	53	–73	[8a]
SH^-	1.7×10^2	30	–100	[9]
SR^- (cys)	2.6×10^4[b]	31	–54	[10]

[a] T = 25 °C, I = 1 M. [b] pH = 9.2. The reported rate constants in ref.[5] correspond to the reaction of the neutral amines. [c] Calculated from the reported data. [d] Value calculated at pH 8 from the third-order rate law.

Equations (10) and (11) describe a stoichiometry similar to that in Equation (1), although reaction (11) differs by the formation of an isolable nitroso derivative.[13] A common characteristic of reactions (1), (10), and (11) is that the adducts cannot be detected. It becomes evident that the N_2O release must be associated with *both* N–H deprotonations in reaction (10),[24] an impossible event in reaction (11), which favors the formation of $CH_3N(NO)OH$. The mechanism for the reactions involves the relatively slow formation of an adduct intermediate between the nitrosyl complex and the nucleophile, followed by easily reversible deprotonations. For NH_2OH, the release of three hydrogen atoms is a requisite for product formation, taking into account that the O–H dissociation should be an activated process, as required by the rate law. Thus, the formation and rapid release of $^{15}NN^{18}O$ ensues, oxygen and central nitrogen coming from the nucleophile. This process comprises the formation of a η^1-N_2O intermediate,[6] which appears to be energetically favorable, with minimal reorganization requirements.[16]

The results for the reaction of SNP with NH_2OCH_3 appear to be notoriously contrasting to those with NH_2OH. As stated above, a second-order rate law describes the overall process for reaction (1), that is, the rate is pH-independent. Table 3 shows another difference: at a given pH, the rate constant for NH_2OCH_3 is much lower than those for NH_2OH and $NHCH_3OH$. Whilst the activation entropies for reactions (10) and (11) are comparatively small (–32 and –13 J K^{-1} mol^{-1}, Table 3), the activation entropy for reaction (1), –220 J K^{-1} mol^{-1}, is much more negative. Also very significant is the different labeling of N_2O in Equation (1), which point to important mechanistic differences with respect to NH_2OH. The production of $N^{15}NO$ requires the movement of the nitrosyl group and the consequent formation of an η^2-N_2O intermediate (Figure 1). The results in Table 3 suggest a similar interpretation for primary amines and for hydrazine. In fact, the side-on η^2-N_2O intermediate has already been proposed, resulting from the N–N cleavage ensuing from the binding of hydrazine to $[Fe(CN)_5NO]^{2-}$, with concomitant formation of NH_3.[7] Moreover, the previous calculations also suggest that the side-on intermediate evolves to the end-on isomer before N_2O release.[16]

When a CH_3 substituent binds to oxygen, only the facile deprotonation of the N-bound hydrogen atoms is feasible. In the absence of an O–H bond (no requirements for O–H activation), the pH-independent rate-law becomes consistent. The release of CH_3OH comprises the cleavage of the N–O bond, aided by proton transfer. We consider that differential rates of migration of H have a crucial role in the rate-limiting formation of the first intermediate, I1, as proposed in reactions (3)–(5), thus accounting for the highly negative activation entropy. It is worth to point out that the same differences in stoichiometry and N_2O labeling also occur for the reactions of NH_2OCH_3 and NH_2OH with nitrous acid.[25]

Conclusions

By discussing the kinetic results for NH_2OCH_3 and other nitrogen hydrides (NH_2OH, $NH(CH_3)OH$, N_2H_4, amines), OH^-, and thiolates together, we provide a comprehensive set of experimental and theoretical evidence on the mechanisms of the addition reactions with NO^+ complexes and the subsequent decomposition reactions. There are different reaction stoichiometries for each nitrogen hydride, leading to the alternative formation of N_2, N_2O, or mixtures of them, together with H_2O, CH_3OH, or NH_3 as additional products. Moreover, there is a common, general mechanistic basis for describing the underlying reactivity, implying an initial reversible addition step with the formation of a covalent bond between the nitrogen atom of the hydrides and the nitrogen atom of the NO^+ group. The detailed

 © 2012 Wiley-VCH Verlag GmbH & Co. KGaA, Weinheim

mechanisms may involve different relative rates of these adduct-formation reactions and the ensuing reorganizations comprising N and/or O-deprotonations, bond cleavages, and the formation of experimentally elusive intermediates. Noticeably, different mechanistic insights arise for NH_2OH and its substituted derivatives, depending on the nature of the (H or alkyl) substituent and its position (on either N or O). We provide theoretical and experimental evidence on the formation of an η^2-N_2O intermediate, as a precursor for N_2O release, when NH_2OCH_3 is the reactant. Other nucleophiles react through the formation of η^1-intermediates, as is the case for NH_2OH. These N_2O intermediates are reminiscent of the well-characterized nitrosyl linkage isomers.[26]

Experimental Section

Materials and Methods

O-Methylhydroxylamine as the hydrochloride salt, NH_2OCH_3·HCl (methoxyamine hydrochloride), and isonicotinamide ($pyCONH_2$) were from Sigma–Aldrich. Dimethyl sulfoxide (DMSO) was from Sintorgan. Sodium pentacyanonitrosylferrate(II) dihydrate ($Na_2[Fe(CN)_5NO]\cdot 2H_2O$, SNP) was from Merck. ^{15}N-labeled sodium nitroprusside was prepared as described in the literature,[27] by using $Na^{15}NO_2$ (99 atom-% ^{15}N) from Isotec. NH_2OCH_3 was dried and stored in a desiccator over silica gel. All other chemicals were analytical or reagent grade and were used without further purification. All solutions were prepared by using deionized water.

Solid K_2HPO_4 or borax were used for preparing 20 mM buffered solutions, and NaCl was added to attain an ionic strength of I = 1 M. The pH was adjusted to the desired value in the range 6.0–9.3 ± 0.1 by using a concentrated solution of HCl. Measurements were performed with a Hanna HI 9231 pH-meter, supplied with a Hanna HI 1131B glass-body combination electrode, calibrated against Merck standard buffers.

Concentrated solutions of NH_2OCH_3 (ca. 500 mM) were prepared by dissolving weighed amounts of NH_2OCH_3·HCl in the buffered solution and readjusting the pH with solid NaOH. According to the pK_a (4.6) for $NH_3OCH_3^+$,[28] we estimate that NH_2OCH_3 is dominant in our reaction conditions. Concentrated solutions of the $[Fe(CN)_5NO]^{2-}$ ion (ca. 200 mM) were generated by dissolving weighed amounts of SNP in deoxygenated buffer solutions.

Kinetic studies at different pH values were mainly performed at 25 ± 0.2 °C under pseudo-first-order conditions in NH_2OCH_3, by using spectrophotometer cells of 1 or 0.1 cm path length. At a pH of about 7.1, we used the temperature range 14–41 °C for obtaining activation parameters through Eyring plots. In a typical kinetic run, an aliquot of NH_2OCH_3 was added to a mixture of SNP and $pyCONH_2$ (50–250 mM). The final reactant concentrations span the range reported in Table 1. The product $[Fe^{II}(CN)_5H_2O]^{3-}$ (λ_{max} = 440 nm, ε_{max} = 640 $M^{-1}cm^{-1}$)[29] forms the stable complex $[Fe^{II}(CN)_5(pyCONH_2)]^{3-}$ (λ_{max} = 435 nm, ε_{max} = 4570 $M^{-1}cm^{-1}$).[20] In this way, the aqua ion can be excluded from the medium, precluding its further reactivity toward NH_2OCH_3, and the sensitivity of product detection is enhanced.[12] The build-up of $[Fe^{II}(CN)_5(pyCONH_2)]^{3-}$ was monitored with a Hitachi U-3210 UV/Vis spectrophotometer in the range 200–900 nm. The quoted rate constants are the average of at least three runs. Additionally, we carried out some kinetic experiments by using ATR spectroscopy, by measuring the decrease in the absorbance of the strong NO stretching mode of SNP at about 1935 cm^{-1},[18] as well as by monitoring the increase of the pressure ensuing from the production of N_2O (see below). FTIR/ATR spectra, spanning the 850–1550 and 1750–3100 cm^{-1} ranges, were recorded with a Perkin–Elmer Spectrum BX spectrophotometer, equipped with standard pre-mounted horizontal ATR accessory with a flat sampling plate of ZnSe. Argon-saturated buffered solutions of the reactants (50–100 mM) were transferred into the plate with a syringe. The spectral output consisted of differences from buffered SNP or NH_2OCH_3 solutions. An excess of DMSO was used as a scavenger of produced $[Fe^{II}(CN)_5H_2O]^{3-}$, through the formation of colorless $[Fe^{II}(CN)_5(DMSO)]^{3-}$.[30]

EPR spectroscopy was employed for the characterization of eventually formed radical transients by using a Bruker ER 200D X-band spectrometer, operated at about 9.78 GHz with a 100 kHz modulation frequency and 1.25 mT modulation amplitude. The central field and the correct operating frequency were calibrated with regard to 4 μM TEMPO (a_N = 1.72 mT; g = 2.0051), used as external standard. The control of signal production was performed under NH_2OCH_3 pseudo-first-order conditions at room temperature, by using a 0.3 cm^3 quartz flow flat cell connected to a homemade stopped-flow accessory.

Gas production was quantitatively measured in a thermostatted, well-stirred closed reactor (0.082 dm^3) linked to an Extrel Emba II mass spectrometer operated at 70 eV. This setup was also equipped with an MKS Model 622 absolute transducer for recording the total pressure.[2a] By using deoxygenated buffer solutions, NH_2OCH_3 (0.010 dm^3) was added to $[Fe(CN)_5NO]^{2-}$ (0.035 dm^3) containing excess DMSO as scavenger. The time evolution of the pressure was recorded continuously, and the mass spectra of the gases in the reactor headspace were acquired at the end of the reaction. CH_3OH was extracted from the exhausted mixtures by distillation; it was characterized and quantified as CH_2O, with the chromotropic acid test.[31] The data were treated by using standard processing software.

Theoretical Calculations: DFT calculations were performed by using a previously described methodology.[16] Briefly, geometry optimization of all intermediate complexes and transition states were carried out by using the B3LYP functional with LANL2DZ basis on the metal atom and 6-31++G* on the other atoms. The structures were fully optimized with no symmetry constraints. The true nature of the optimized minima in the gas phase has been verified in each case by calculating the harmonic frequencies. Transition states were fully characterized by means of a vibrational analysis, leading to one imaginary frequency. The solvent (water) effect was considered in terms of the isodensity polarizable continuous model (IPCM). For the optimized structures, we calculated thermodynamic functions at 298 K and 1 bar by using standard statistical thermodynamic methods based on the rigid-rotor harmonic oscillator approximations.

Supporting Information (see footnote on the first page of this article): Eyring plot of the average rate constants, k_{exp}, at various temperatures and their numerical values.

Acknowledgments

We thank the University of Buenos Aires, the University of Mar del Plata, the Agencia Nacional de Promoción Científica y Tecnológica (ANPCYT), and the Consejo Nacional de Investigaciones Científicas y Técnicas (CONICET) for support. V. T. A. and J. A. O. are members of the scientific staff of CONICET.

 © 2012 Wiley-VCH Verlag GmbH & Co. KGaA, Weinheim

[1] a) I. M. Wasser, S. de Vries, P. Moënne-Loccoz, I. Schröder, K. D. Karlin, *Chem. Rev.* **2002**, *102*, 1201; b) J. N. Armor (Ed.), *Environmental Catalysis, ACS Symp. Ser., Volume 552*, **1994**.

[2] a) J. A. Olabe, L. D. Slep in *Comprehensive Coordination Chemistry II, From Biology to Nanotechnology* (Eds.: J. A. Mc Cleverty, T. J. Meyer), Elsevier, Oxford, **2004**, vol. 1, p. 603; b) J. A. Olabe, *Adv. Inorg. Chem.* **2004**, *55*, 61; c) L. J. Ignarro (Ed.), *Nitric Oxide, Biology and Pathobiology*, Academic Press, San Diego, CA, **2000**.

[3] a) J. A. Olabe, *Dalton Trans.* **2008**, 3633; b) F. Roncaroli, M. Videla, L. D. Slep, J. A. Olabe, *Coord. Chem. Rev.* **2007**, *251*, 1903; c) A. R. Butler, I. L. Megson, *Chem. Rev.* **2002**, *102*, 1155.

[4] a) N. E. Katz, M. A. Blesa, J. A. Olabe, P. J. Aymonino, *J. Inorg. Nucl. Chem.* **1980**, *42*, 581; b) I. Maciejowska, Z. Stasicka, G. Stochel, R. van Eldik, *J. Chem. Soc., Dalton Trans.* **1999**, 3643.

[5] L. Dozsa, V. Kormos, M. T. Beck, *Inorg. Chim. Acta* **1984**, *82*, 69.

[6] S. K. Wolfe, C. Andrade, J. H. Swinehart, *Inorg. Chem.* **1974**, *13*, 2567.

[7] M. M. Gutiérrez, V. T. Amorebieta, G. L. Estiú, J. A. Olabe, *J. Am. Chem. Soc.* **2002**, *124*, 10307.

[8] a) J. H. Swinehart, P. A. Rock, *Inorg. Chem.* **1966**, *5*, 573; b) J. Masek, H. Wendt, *Inorg. Chim. Acta* **1969**, *3*, 455.

[9] a) P. A. Rock, J. H. Swinehart, *Inorg. Chem.* **1966**, *5*, 1078; b) S. L. Quiroga, A. E. Almaraz, V. T. Amorebieta, L. L. Perissinotti, J. A. Olabe, *Chem. Eur. J.* **2011**, *17*, 4145.

[10] a) M. D. Johnson, R. G. Wilkins, *Inorg. Chem.* **1984**, *23*, 231; b) K. Szacilowski, A. Wanat, A. Barbieri, E. Wasielewska, M. Witko, G. Stochel, Z. Stasicka, *New J. Chem.* **2002**, *26*, 1495.

[11] K. Wieghardt, *Adv. Inorg. Bioinorg. Mech.* **1984**, *3*, 213.

[12] a) I. Choi, Y. Liu, Z. Wei, M. D. Ryan, *Inorg. Chem.* **1997**, *36*, 3113; b) G. Alluisetti, A. E. Almaraz, V. T. Amorebieta, F. Doctorovich, J. A. Olabe, *J. Am. Chem. Soc.* **2004**, *126*, 13432; c) M. M. Gutiérrez, G. B. Alluisetti, C. Gaviglio, F. Doctorovich, J. A. Olabe, V. T. Amorebieta, *Dalton Trans.* **2009**, 1187; d) M. M. Gutiérrez, J. A. Olabe, V. T. Amorebieta, *Inorg. Chem.* **2011**, *50*, 8817.

[13] M. M. Gutiérrez, G. B. Alluisetti, J. A. Olabe, V. T. Amorebieta, *Dalton Trans.* **2008**, 5025.

[14] M. Feelisch, J. S. Stamler (Eds.), *Methods in Nitric Oxide Research*, John Wiley and Sons, Chichester, **1996**.

[15] a) D. Benoit, V. Chaplinski, R. Braslau, C. J. Hawker, *J. Am. Chem. Soc.* **1999**, *121*, 3904; b) P. Marsal, M. Roche, P. Tordo, P. Sainte Claire, *J. Phys. Chem. A* **1999**, *103*, 2899; c) D. K. Kim, Y. W. Kim, K. H. Kim, *J. Heterocycl. Chem.* **1997**, *34*, 311; d) Z. Gdaniec, B. Ban, L. C. Sowers, G. V. Fazakerley, *Eur. J. Biochem.* **1996**, *242*, 271; e) C. Buschfort, M. R. Muller, S. Seeber, M. F. Rajewski, J. Thomale, *Cancer Res.* **1997**, *57*, 651; f) M. Liuzzi, M. Talpaert-Borle, *J. Biol. Chem.* **1985**, *260*, 5252; g) L. Liu, P. Taverna, C. M. Whitacre, S. Chatterjee, S. L. Gerson, *Clin. Cancer Res.* **1999**, *5*, 2908; h) P. Taverna, H. S. Hwang, J. E. Schupp, T. Radivoyevitch, N. N. Session, D. A. Zarling, T. J. Kinsella, *J. Cancer Res.* **2003**, *63*, 838; i) M. She, I. Pan, L. Sun, S. C. Yeung, *Leukemia* **2003**, *19*, 595.

[16] J. A. Olabe, G. L. Estiú, *Inorg. Chem.* **2003**, *42*, 4873.

[17] The central ^{15}N label is demonstrated by the analysis of the fragmentation spectrum of N_2O (cf. foot-note 32 in Ref.[7]).

[18] J. D. Schwane, M. T. Ashby, *J. Am. Chem. Soc.* **2002**, *124*, 6822.

[19] N. G. del V. Moreno, N. E. Katz, J. A. Olabe, P. J. Aymonino, *Inorg. Chim. Acta* **1978**, *35*, 183.

[20] a) H. E. Toma, J. M. Malin, *Inorg. Chem.* **1973**, *12*, 1039; b) H. E. Toma, J. M. Malin, *Inorg. Chem.* **1973**, *12*, 2080.

[21] R. G. Wilkins, *Kinetics and Mechanisms of Reactions of Transition Metal Complexes*, 2nd ed., VCH Verlag, Weinheim, Germany, **1992**.

[22] Our calculations focus on the structural characterization of the stable species appearing along the reaction pathway, without attempting a more complex (exhaustive) kinetic study, which should include a more thorough consideration of environmental and thermodynamic contributions. In this context, the results with the IPCM model reveal numerical changes in the values of the activation parameters (particularly enthalpies) by using alternative localizations of water molecules hydrogen-bonded to the hydrogen atoms of the NH_2 group in NH_2OCH_3. We are still searching for an adequate theoretical tool for the computation of the specific solvent effects. The structural results derived from the geometry optimization process could also be influenced by these limitations, although the gross geometrical features of the N_2O intermediates have already been reported in ref.[16]

[23] F. Roncaroli, M. E. Ruggiero, D. W. Franco, G. L. Estiu, J. A. Olabe, *Inorg. Chem.* **2002**, *41*, 5760.

[24] The reported unreactivity of *N*,*N*′-dimethylhydroxylamine toward addition in $[Fe(CN)_5NO]^{2-}$ (ref.[13]) constitutes good evidence on the proton-releasing requirements. Similar unreactivity occurs with 1,1-dimethylhydrazine, when binding through the NMe_2 group (ref.[7]).

[25] J. E. Leffler, A. A. Bothner, *J. Am. Chem. Soc.* **1951**, *73*, 5473.

[26] M. D. Carducci, M. R. Pressprich, P. Coppens, *J. Am. Chem. Soc.* **1997**, *119*, 2669.

[27] M. E. Chacón Villalba, E. L. Varetti, P. J. Aymonino, *Vib. Spectrosc.* **1997**, *14*, *275*.

[28] T. C. Bissot, R. W. Parry, D. H. Campbell, *J. Am. Chem. Soc.* **1957**, *79*, 796.

[29] H. E. Toma, *Inorg. Chim. Acta* **1975**, *15*, 205.

[30] H. E. Toma, J. M. Malin, E. Giesbrecht, *Inorg. Chem.* **1973**, *12*, 2084.

[31] a) R. N. Boos, *Anal. Chem.* **1948**, *20*, 964; b) *NIOSH Manual of Analytical Methods*, Method No. 3500, 4th ed., **1994**.

Received: April 18, 2012
Published Online: August 24, 2012

 © 2012 Wiley-VCH Verlag GmbH & Co. KGaA, Weinheim